

ARTICLE

Assessing CYP2C19 Ontogeny in Neonates and Infants Using Physiologically Based Pharmacokinetic Models: Impact of Enzyme Maturation Versus Inhibition

Peng Duan¹, Fang Wu¹, Jason N. Moore², Jeffrey Fisher³, Victor Crensil⁴, Daniel Gonzalez⁵, Lei Zhang⁶, Gilbert J. Burckart² and Jian Wang^{7,*}

The objective of this study was to develop pediatric physiologically based pharmacokinetic (PBPK) models for pantoprazole and esomeprazole. Pediatric PBPK models were developed by Simcyp version 15 by incorporating cytochrome P450 (CYP)2C19 maturation and auto-inhibition. The predicted-to-observed pantoprazole clearance (CL) ratio ranged from 0.96–1.35 in children 1–17 years of age and 0.43–0.70 in term infants. The predicted-to-observed esomeprazole CL ratio ranged from 1.08–1.50 for children 6–17 years of age, and 0.15–0.33 for infants. The prediction was markedly improved by assuming no auto-inhibition of esomeprazole in infants in the PBPK model. Our results suggested that the CYP2C19 auto-inhibition model was appropriate for esomeprazole in adults and older children but could not be directly extended to infants. A better understanding of the complex interplay of enzyme maturation, inhibition, and compensatory mechanisms for CYP2C19 is necessary for PBPK modeling in infants.

Study Highlights

WHAT IS THE CURRENT KNOWLEDGE ON THE TOPIC?

✓ Understanding CYP2C19 ontogeny is important for optimal prediction of pediatric safety and effectiveness of drugs that are substrates or interact with CYP2C19, but enzyme auto-inhibition has not been investigated in neonates and infants.

WHAT QUESTION DID THIS STUDY ADDRESS?

✓ Pantoprazole and esomeprazole share the CYP2C19 pathway but differ in their inhibition property on CYP2C19. Our PBPK study found that CL predictions for pantoprazole were within the twofold range for pediatrics, whereas the esomeprazole PBPK model significantly underpredicted CL in neonates and infants.

WHAT DOES THIS STUDY ADD TO OUR KNOWLEDGE?

✓ The esomeprazole PBPK model with CYP2C19 auto-inhibition could not be applied to neonates/infant. A better prediction without CYP2C19 auto-inhibition, suggests that the interplay of CYP maturation and inhibition in the neonates and infants might be age-dependent.

HOW MIGHT THIS CHANGE DRUG DISCOVERY, DEVELOPMENT, AND/OR THERAPEUTICS?

✓ Application of PBPK modeling to inform drug exposure in pediatrics requires an understanding of mechanisms that alter drug CL, such as the interplay of enzyme inhibition and maturation as well as the possible compensatory pathways.

Pediatric populations undergo major growth-related physiological changes that are known to alter drug disposition. For example, compared to adults, infant or neonate hepatic and renal clearance systems are immature, particularly in the first few weeks of life.¹ Therefore, there is the need to characterize the pharmacokinetics (PKs) of drugs used

in pediatric patients, especially neonates and infants, to ensure that the benefit/risk is optimized for these vulnerable patient populations. In spite of the need for pediatric PK data to inform dosing, prospective studies are difficult to perform in younger children, resulting in a scarcity of data.^{2,3} Some of the challenges in conducting PK studies

¹Office of New Drug Product, Office of Pharmaceutical Quality, Center for Drug Evaluation and Research, Food and Drug Administration, Silver Spring, Maryland, USA;

²Office of Clinical Pharmacology, Office of Translational Sciences, Center for Drug Evaluation and Research, Food and Drug Administration, Silver Spring, Maryland, USA;

³Division of Biochemical Toxicology, National Center for Toxicological Research, Jefferson, Arkansas, USA; ⁴Office of Drug Evaluation III, Office of New Drugs, Center for Drug Evaluation and Research, Food and Drug Administration, Silver Spring, Maryland, USA; ⁵Division of Pharmacotherapy and Experimental Therapeutics, UNC Eshelman School of Pharmacy, University of North Carolina at Chapel Hill, Chapel Hill, North Carolina, USA; ⁶Office of Research and Standards, Office of Generic Drugs, Center for Drug Evaluation and Research, Food and Drug Administration, Silver Spring, Maryland, USA; ⁷Office of Drug Evaluation IV, Office of New Drugs, Center for Drug Evaluation and Research, Food and Drug Administration, Silver Spring, Maryland, USA. *Correspondence: Jian Wang (jian.wang@fda.hhs.gov)

in pediatric patients include intense PK sample collection schemes that are typically not feasible, parental consent rates for these studies that are often low, and ethical concerns that are enhanced by the difficulty in demonstrating the potential for direct benefit for infants enrolled in clinical studies.⁴ To circumvent these challenges, modeling and simulation that leverages existing knowledge can be used to fill the knowledge gap.⁵ Among the modeling and simulation approaches, physiologically based pharmacokinetic (PBPK) modeling is emerging as a method that is particularly attractive because it can incorporate pediatric physiology that may be undergoing changes during growth and development in conjunction with enzyme/transporter ontogeny to improve the accuracy of predicting drug exposure.^{3,6–10}

Cytochrome P450 (CYP)2C19 is an important drug-metabolizing enzyme, and knowledge of the influence of CYP2C19 is critical in pediatric pharmacology for understanding drug disposition. Despite its importance in drug metabolism, CYP2C19 expression reaches no more than 15% of mature levels throughout the prenatal period and its expression increases linearly in the first 5 postnatal months.¹¹ In addition to CYP2C19 ontogeny, genetic polymorphisms are also important predictors of drug clearance, and must be accounted for in models used to characterize disposition of CYP2C19 substrates.¹²

The objective of this study was to use PBPK models to help understand CYP2C19 maturation and inhibition using two probe substrates, pantoprazole and esomeprazole, in pediatric patients through a learn-confirm-refine strategy. Both drugs are extensively metabolized in the liver through demethylation by CYP2C19 with subsequent sulfation and minor oxidation by CYP3A4. However, esomeprazole is an inhibitor of CYP2C19, whereas pantoprazole is not.^{13,14} Once these models are developed, a similar approach could be used to predict the exposure of other drugs metabolized by CYP2C19 in infants.

METHODS

The exploration of CYP2C19 maturation followed a learn-confirm-refine strategy for each PBPK model. The workflow for pantoprazole and esomeprazole PBPK models used for pediatrics is described in **Figure 1**.^{15,16} All the PBPK models were developed in Simcyp version 15 (Certara).

Development of adult PBPK models

For pantoprazole, first, an adult model was developed and the intrinsic clearance of CYP2C19 and CYP3A4 was optimized, as shown below, by using the published plasma concentration vs. time data collected following a 20 mg i.v. infusion or a 40 mg single oral dose of pantoprazole.¹⁷ The adult model was verified by simulating the pantoprazole plasma concentration vs. time data for different CYP2C19 genotypes and comparing them to the observed data.¹⁸ Pantoprazole area under the plasma concentration-time curve (AUC), maximal concentration (C_{max}), and clearance (CL) values for each subject were estimated

by noncompartmental analysis (Phoenix WinNonlin 6.4). **Table 1** lists the drug-dependent parameters for the final pantoprazole PBPK model. The drug absorption of pantoprazole was predicted using the advanced distribution, absorption, and metabolism model and apparent permeability measured in Caco-2 cell lines.¹⁹ The formulation parameters were obtained from the literature.²⁰ The predicted $\log P_{vo:w}$ (the logarithm of the olive oil: buffer distribution coefficient at pH 7.4) was 1.326. The predicted volume of distribution at steady state (obtained using tissue volumes for a population representative of healthy volunteers) was 0.095 L/kg by the Rodgers and Rowland equation.^{21,22} Renal CL of pantoprazole was 0.0012 L/hour, which was calculated as the product of plasma fraction unbound and the urine flow, which were 0.02 and 1 mL/minute, respectively.^{14,23} Pantoprazole is predominantly metabolized by CYP2C19, with only a small fraction metabolized by CYP3A4.^{14,24} The contribution percentage of each CYP isoform has not been previously reported. Pantoprazole's adult CL following i.v. administration was reported as ~15 L/hour.^{14,25} The automatic sensitivity analysis and parameter estimation²⁶ modules were used to estimate the intrinsic CL (CL_{int}) of CYP2C19 and CYP3A4 by fitting against the plasma concentration vs. time data following a 20 mg i.v. dose and observed pantoprazole clearance.¹⁷ The estimated CL_{int} of CYP2C19 was 17.6 $\mu\text{L}/\text{minute}/\text{pmol}$, whereas the CL_{int} of CYP3A4 was 0.1996 $\mu\text{L}/\text{minute}/\text{pmol}$. With these CL_{int} values and retrograde model tool in Simcyp, CYP2C19 contributed around 90% of pantoprazole metabolism, whereas CYP3A4 contributed the rest (~10%), which is consistent with the drug product labeling.²⁷

The esomeprazole PBPK model in the Simcyp repository was used, which was published previously.²⁸ **Table 1** provides the input parameters for the final esomeprazole PBPK model. The auto-inhibition involved in esomeprazole clearance was modeled using both reversible and irreversible inhibition of CYP2C19 (i.e., time-dependent inhibition (TDI)).²⁹ However, the main contribution to auto-inhibition for esomeprazole is from irreversible inhibition (i.e., TDI) are the maximal inactivation rate constant (k_{inact}), the inhibitor concentration causing half-maximal inactivation (K_i), and the apparent first-order degradation rate constant for the enzyme *in vivo* (k_{deg}). The software default values of $k_{deg,CYP2C19}$ are 0.0267 and 0.03/hour for the liver and gut, respectively. As a result of auto-inhibition of CYP2C19 (via TDI), time-variant intrinsic metabolic clearance of the drug by CYP2C19 in organs ($CL_{U,int,organ,CYP2C19}$) value becomes time-dependent in both the gut and the liver. Note that in the base/initial model, time-variant intrinsic metabolic clearance of the drug ($CL_{U,int}$) was obtained from retrograde, which may not be the "true" estimate of $CL_{U,int}$. Sensitivity analyses were conducted to explore plausible combinations of $CL_{U,int,organ,CYP2C19}$, K_i , and k_{inact} of CYP2C19 for esomeprazole using human PK data from various sources. Specifically, the $CL_{U,int,organ,CYP2C19}$ at the enzyme level was fixed at three different levels (16.2, 24.3, and 32.4 $\mu\text{L}/\text{minute}/\text{pmol}$ of isoform; refer to the supporting information of the publication²⁸) and a sensitivity analysis on K_i and k_{inact} was performed at each fixed level of intrinsic CL value. The best parameter values for $CL_{U,int,organ,CYP2C19}$, K_i ,

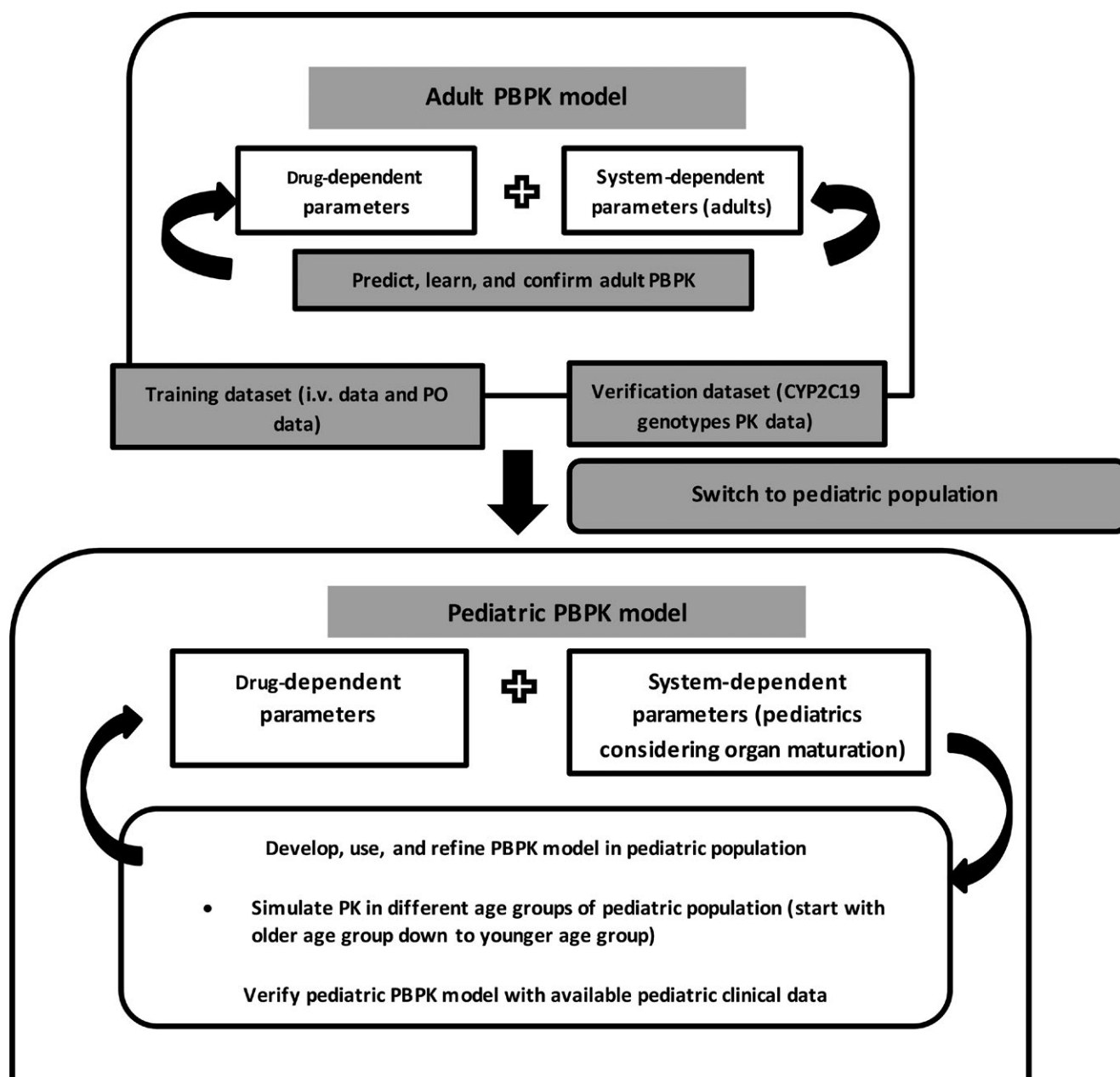


Figure 1 Modeling flowchart for pantoprazole and esomeprazole pediatric physiologically based pharmacokinetic (PBPK) model.^{8,15,16} CYP, cytochrome P450; PK, pharmacokinetic.

and k_{inact} were selected for the final model for esomeprazole by comparing the simulated PK profiles and parameters to the observed ones for i.v. and oral PK data. The kinetic parameter describing the reversible inhibition is K_i . The K_i of CYP2C19 used in the PBPK model is 7.5 μM , assumed as half-maximal inhibitory concentration (IC_{50})/2 (competitive/reversible inhibition), where IC_{50} value = 15 μM .²⁹

Pediatric PBPK models

The adult PBPK models for pantoprazole and esomeprazole were extended by using the age-dependent changes of anatomic and physiological parameters (Simcyp version 15 default parameters) to predict pantoprazole exposure

across different age groups in a stepwise manner (starting with adolescents and then extending to children, infants, and neonates, respectively).^{30–33} Equations 1 and 2 describe the enzyme ontogeny of hepatic CYP2C19 and CYP3A4 with Simcyp default parameters, respectively.³⁴

$$\text{CYP2C19 fraction of adult expression} = \frac{(\text{Adult}_{\max} - F_{\text{birth}}) * \text{Age}^n}{\text{Age}_{50}^n + \text{Age}^n} + F_{\text{birth}} \quad (1)$$

Where Adult_{\max} (maximum adult expression) is 0.98; F_{birth} (fractional expression at birth relative to adult) is 0.3; Age_{50} (time to half adult expression) is 0.29; Age is the postnatal age in

Table 1 Drug-dependent parameters for the pantoprazole and esomeprazole PBPK model

Parameters	Pantoprazole	Reference	Esomeprazole	Reference
Molecular weight (g/mol)	432.4	ChEMBL	345.4	Simcyp library ^a
LogP _{o/w}	2.4	PubChem	2.23	Simcyp library ^a
Compound type	Monoprotic acid	PubChem	Ampholyte	Simcyp library ^a
pK _a	3.92	PubChem	4.4, 8.7	Simcyp library ^a
Blood/plasma	0.55	47	0.59	Simcyp library ^a
F _u	0.02	14	0.03	b
Absorption model:	ADAM	19	Absorption model:	
pH 6.5:7.4: Caco-2 (10 ⁻⁶ cm/second)	18.3		K _a (L/hour): 10	c
P _{eff,man} (10 ⁻⁴ cm/second)	3.329 (Predicted)		F _g : 1 Q _{gut} (L/hour): 6	d Predicted by SimCYP
Distribution model:	Full PBPK model	14	F _{u,gut} : 0.03 Minimal PBPK: V _{ss} (L/kg): 0.2	Same as f _{up} 48
Elimination model:	Enzyme kinetics:		Enzyme kinetics:	
	CL _{int} of CYP2C19: 17.57602 (μL/minute/pmol of isoform)	Sensitivity analysis and parameter estimate by fitting to clinically observed 20 mg i.v.	CL _{int} of CYP2C19: 24.3 (μL/minute/pmol of isoform)	e
	CL _{int} of CYP3A4: 0.1996 (μL/minute/pmol of isoform)		CL _{int} of CYP3A4: 0.36 μL/minute/pmol of isoform)	e
			f _m of CYP2C19 (%): 73% f _m of CYP3A4 (%): 27%	49
			F _{u,mic} : 1	f
	CL _R (L/hour): 0.0012	23	CL _R (L/hour): 0.037	a
Enzyme interaction:	N/A		For irreversible inhibition K _i of CYP2C19 (μM): 0.3 K _{inact} of CYP2C19 (L/hour): 5	g
			For reversible inhibition: Ki CYP2C19 (μM): 7.5	Assume Ki = IC _{50/2} , IC ₅₀ value = 15 μM ³⁰
Formulation parameters				
Solid formulation: Enteric coated tablets or granules	Triggering pH = 6.8	20	Solution	
Intrinsic solubility (mg/mL)	0.05	PubChem		

ADAM, advanced dissolution, absorption, and metabolism; ChEMBL, European Bioinformatics Institute; CL_{int}, intrinsic clearance of enzyme; CL_R, renal clearance; CYP, cytochrome P450; f_a, fraction available from dosage form; f_g, the fraction of drug that escapes first pass metabolism in the gut; f_m, the relative contribution (f_m) of the various elimination pathways for a drug; f_{u,gut}, unbound fraction of drug in enterocytes f_{u,mic}, unbound fraction in microsome; IC₅₀, half-maximal inhibitory concentration; k_a, absorption rate constant (1/hour); Ki, concentration of inhibitor that supports half maximal inhibition (μM) for reversible inhibition; K_i, concentration of inhibitor that supports half maximal inhibition (μM) for irreversible inhibition; K_{inact}, inactivation rate of enzyme (L/hour); LogP_{o/w}, logarithm of the n-octanol:buffer partition coefficient; N/A, not applicable; Q_{gut}, a nominal flow in gut model (L/hour; P_{eff,man}, effective permeability in man); V_{ss}, volume of distribution at steady state (L/kg).

^aAssumed same as omeprazole, obtained from Simcyp compound library. ^bLabel of Esomeprazole obtained from Drugs@FDA, <http://www.accessdata.fda.gov/scripts/cder/drugsatfda/>. ^cParameter estimated using Phoenix WinNonlin by compartmental analysis of phase I data⁵⁰. It was assumed that 100% fraction of dose can be absorbed into enterocytes from solution. ^dGut metabolism is considered negligible. ^eRetrograde calculated value based on observed CL_{iv} (L/hour) after 20 mg single dosing of esomeprazole⁴⁹. ^fSimcyp compound library for omeprazole and model prediction. ^gSensitivity analysis and value of omeprazole²⁹.

years; the “n” in Ageⁿ is 2.44; and the age cutoff is 5 years (adult expression for CYP2C19 is used for children > 5 years of age).

Eq. 2a describes adult expression for CYP3A4 for age groups ≤ 25 years of age, and age is in units of years, whereas Adult_{max} is 1.06, F_{birth} is 0.11, Age₅0ⁿ is 0.64, the “n” in Ageⁿ is 1.91.

$$\text{CYP3A4 fraction of adult expression} = \frac{(\text{Adult}_{\text{max}} - F_{\text{birth}}) * \text{Age}^n}{\text{Age}_{50}^n + \text{Age}^n} + F_{\text{birth}} \quad (2a)$$

(For age groups ≤ 25 years of age).³⁴ Eq. 2b³⁴ describes the adult expression for CYP3A4 for age groups > 25 years of age, and age is in units of years.

$$\text{CYP3A4 fraction of adult expression} = -0.12274 * \exp^{-0.05 * (\text{Age} - 2.2)} + 1.1 \quad (2b)$$

CYP2C19 and CYP3A4 are also expressed in the intestine. The ontogeny equations for intestinal CYP2C19 and CYP3A4 are the same as the respective hepatic enzyme (Eqs. 1 and 2, respectively), but the parameter values are different. For intestinal CYP3A4 and CYP2C19, the parameters are: Adult_{max}, 1.059; F_{birth}, 0.42; Age₅0ⁿ is 2.357; the “n” in Age₅0ⁿ is 1; and the age cutoff is 18 years (adult expression of CYP2C19 would be used when age is > 18 years; and Eq. 2b will be used for CYP3A4 if age is > 18 years).³⁴

To predict the *in vivo* whole organ hepatic clearance of a drug metabolized by CYPs, the *in vitro* CL_{int} via a CYP enzyme (e.g., obtained with *in vitro* liver microsomes, fresh or cryopreserved hepatocytes, or recombinant enzymes) is scaled by multiplying a series of scaling factors, including milligram of microsomal protein per gram of liver (MPPGL), CYP abundance, and total liver weight.^{35,36} The CYP abundance values in various pediatric age groups are obtained using adult values that are multiplied by an enzyme-specific hepatic ontogeny fraction obtained using the above-described equations (Eqs. 1 and 2). Similarly, the intestinal CL for a drug metabolized by CYPs is obtained by scaling up CL_{int} values for CYP enzymes by multiplying scaling factors, including microsomal protein per whole intestine, and relative CYP abundance in the intestine.^{37,38} In addition to the enzyme ontogeny, age-dependent changes in physiological parameters, such as organ size or volume, age-related plasma protein binding are also incorporated in the model.³⁴

PK simulations in pediatric populations

Virtual population simulations used 10 trials with 50 subjects each (500 subjects in total) for pantoprazole and 10 trials with 10 subjects each (100 subjects in total) for esomeprazole for each age group specified in the figure legends by matching the demographic data of the actual clinical study data (e.g., age, female/male ratio, etc.). The cutoff for each age band, as shown in the figure legends, was based on the available observed data.

PK simulations in different CYP2C19 genotypes

The PK parameters of pantoprazole in a CYP2C19 extensive metabolizer (EM) or in a CYP2C19 poor metabolizer (PM) were simulated and compared with clinical observations from adults (6 subjects of EM and 2 subjects of PM) and pediatric populations (21 subjects of EM and 3 subjects of PM, respectively; **Table S1**). The effect of CYP2C19 polymorphism on the exposure of esomeprazole in the adult population was previously assessed and published by using the same model.²⁸

Evaluation of predictive performance

The predictive performance of each PBPK model was determined by using the ratio (*R*) of simulated CL (CL predicted) to the observed CL (CL observed). The 95% confidence interval (CI) of the ratio of the two means was calculated, as described by Fieller.³⁹ The *R* value was also calculated to evaluate the predictions of other PK parameters, such as AUC and C_{max} . An *R* value within a range of 0.5–2.0 (two-fold) was considered satisfactory.⁴⁰ Furthermore, we considered that the models were acceptable when the clinical observations were between the 95th percentile and 5th percentile of the simulated mean plasma concentration-time curve.⁴¹

RESULTS

Adult PBPK models

The workflow of the modeling was described in **Figure 1**. The predicted pantoprazole plasma concentration vs. time profiles for the adult PBPK model following administration of a 20 mg i.v. infusion and a 40 mg oral delayed-release

tablet were shown in **Figure 2**. Clinical observations were within the within 5th and 95th percentile of the mean simulated concentration, which met one of our predefined model acceptance criteria.^{13,14} The mean ratios (95% CI) of the predicted-to-observed (*R* values) CL estimates were 1.13 (1.04–1.24) and 1.03 (0.74–1.67) for the i.v. and oral data, respectively (**Figure 3a**). In clinical studies of healthy adults who were administered 40 mg orally,¹⁸ the AUC, C_{max} , and CL predicted by the pantoprazole PBPK model for different CYP2C19 genotypes were within twofold compared with clinical observations (**Table S1**). Previous studies have demonstrated that an esomeprazole adult PBPK model incorporating CYP2C19 auto-inhibition could reasonably characterize PK profiles following single and multiple doses.²⁸

Pediatric PBPK models

Pantoprazole

Figure 2 shows the simulated vs. observed pantoprazole plasma concentration-time profiles in neonates, and in children between 1 and 5 years, 6 and 11 years, and 12 and 16 years of age. No observed PK profiles were available for children 1 month to 1 year of age. The clinical observations were generally well aligned with the mean simulated plasma concentration. The model slightly underestimated drug exposure in neonates, but the clinical observations were still between the 95th percentile and 5th percentile of the mean simulated concentration. The *R* values for CL (95% CI) were 1.29 (0.84–1.78) for children 12–16 years of age given 40 mg pantoprazole orally,³⁰ 0.96 (0.70–1.30) for children 6–11 years given 20 mg orally,³⁰ 1.35 (1.25–1.51) for children 1–5 years of age given i.v. infusion of 1.6 mg/kg,³² 0.43 (0.30–0.87) for children 1 month to 1 year of age given 1.25 mg/kg orally,¹⁴ and 0.70 (0.50–0.90) for neonates given 1.25 mg orally (**Figure 3a**, **Tables S2** and **S3**).³³

Pantoprazole exposure was simulated in children between 2 and 14 years of age for both CYP2C19 EM and PM phenotypes using the pediatric PBPK model at a dose of 1 mg/kg pantoprazole. The predicted PK parameters for PM and EM populations were within twofold of the observed values (**Table S1**) with slightly overestimation of C_{max} in the PM population.²⁵

Esomeprazole

Figure 3b shows the *R* values for CL when comparing the PBPK simulated results with reported values in the literature.⁴² We did not overlay the predicted and observed plasma concentration-time profile data for esomeprazole in pediatrics because the above data are not available in the public domain. The esomeprazole pediatric PBPK model with enzyme auto-inhibition reasonably described the clearance after multiple i.v. doses of esomeprazole in patients aged 6–17 years. However, the esomeprazole model underpredicted the CL (overprediction of AUC) for neonates and infants (*R* values for CL ratio were 0.15 and 0.33, respectively). The ratio for AUC was shown in **Table S4**. An improved prediction of AUC ratios, 9.25 (95% CI: 8.16–10.31) with CYP2C19 auto-inhibition, vs. 1.19 (95% CI: 0.592–8.004) without CYP2C19 auto-inhibition, was found for neonates (**Figure 3b**, and **Table S4**). Consistently, the

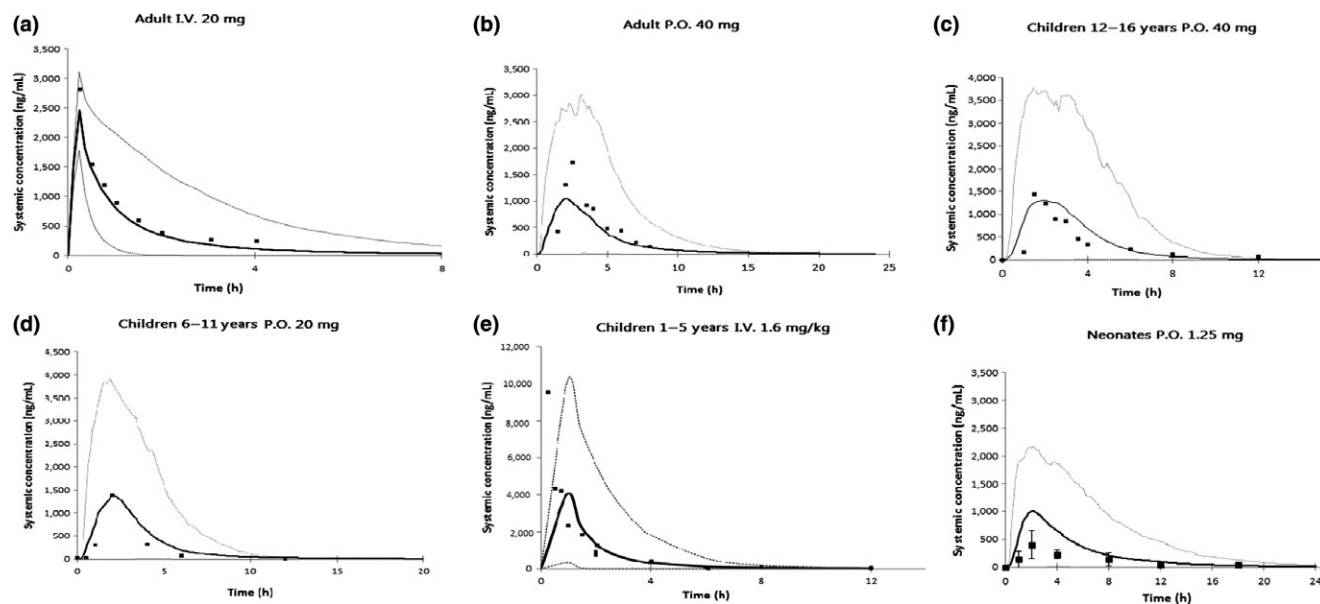


Figure 2 Simulated pantoprazole plasma concentration-time profile after administration of (a) 20 mg i.v. in adult, (b) single oral 40 mg delayed released tablet in adult, (c) single oral 40 mg delayed released tablet in children aged 12–16 years, (d) single oral 20 mg delayed released tablet in children aged 6–11 years, (e) i.v. infusion of 1.6 mg/kg in children aged 1–5 years, (f) single oral 1.25 mg delayed released granules in neonates. (a) Simulated vs. observed plasma time-concentration profile of pantoprazole after i.v. infusion of 20 mg delayed release tablet (subjects = 12).¹⁷ The solid square denotes mean values from the clinical studies. The thick line represents the mean value of the simulated concentration, whereas the thin dash line represents 95th percentile and 5th percentile of simulated plasma concentration. (b) Simulated vs. observed plasma time-concentration profile of pantoprazole after single oral administration of 40 mg delayed release tablet (subjects = 12).¹⁷ The solid square denotes mean values from the clinical studies. The thick line represents the mean values of the simulated concentration, whereas the thin dash curves represent 95th percentile and 5th percentile of simulated plasma concentration, respectively. (c) Simulated vs. observed plasma time-concentration profile of pantoprazole after single oral administration of 40 mg delayed release tablet in children aged 12–16 years (subjects = 11).³⁰ The solid square denotes mean values from the clinical studies. The thick line represents the mean values of the simulated concentration, whereas the thin dash curves represent 95th percentile and 5th percentile of simulated plasma concentration, respectively. (d) Simulated vs. observed plasma time-concentration profile of pantoprazole after single oral administration of 20 mg delayed release tablet in children aged 6–11 years (subjects = 10).³⁰ The solid square denotes mean values from the clinical studies. The thick line represents the mean values of the simulated concentration, whereas the thin dash curves represent 95th percentile and 5th percentile of simulated plasma concentration, respectively. (e) Simulated vs. observed plasma time-concentration profile of pantoprazole after i.v. infusion of 1.6 mg/kg pantoprazole in children aged 1–5 years (subjects = 5).³² The solid squares denote the clinically observed mean plasma concentration sampled at different timepoints from the clinical studies. The thick line represents the mean values of the simulated concentration, whereas the thin dash curves represent 95th percentile and 5th percentile of simulated plasma concentration, respectively. (f) Simulated vs. observed plasma time-concentration profile of pantoprazole after single oral administration of 1.25 mg delayed release granules in neonates (subjects = 14).³³ The solid square with error bar denotes mean values (with SD) from the clinical studies. The thick line represents the mean values of the simulated concentration, whereas the thin dash curves represent 95th percentile and 5th percentile of simulated plasma concentration, respectively.

CL ratio in neonates was 0.15 (95% CI: 0.070–0.29) with CYP2C19 auto-inhibition and was 1.00 (95% CI: 0.575–3.215) when CYP2C19 auto-inhibition was not included. An improved prediction for age groups of 1–12 months and 1–5 years old was also observed when CYP2C19 auto-inhibition was not included in the model.

DISCUSSION

We followed a “learn, confirm, and refine” PBPK modeling strategy by evaluating the PBPK prediction performance with a pediatric pantoprazole model followed by confirming and refining with a pediatric esomeprazole model.¹⁶ These two probe substrates were chosen because esomeprazole is both a substrate and inhibitor of CYP2C19, whereas pantoprazole is only a substrate of CYP2C19. These models were based on a comparison of pantoprazole PK after

single and multiple doses,³³ and a previous model by Wu *et al.*²⁸ in which a CYP2C19 auto-inhibition was considered in an esomeprazole PBPK adult model. Our study found that clearance predictions were within a twofold range for pantoprazole in both the adult and pediatric populations using an established PBPK platform. However, the esomeprazole PBPK model with CYP2C19 auto-inhibition significantly underpredicted CL in the younger age group of pediatric patients, especially in neonates. The differences in PBPK model predictive performance for the two drugs suggest the difficulty in the extrapolation of PK models between drugs sharing an elimination pathway.⁴³ The PBPK model with CYP2C19 auto-inhibition for esomeprazole, which has been verified in adults and older children, could not be directly extrapolated to neonates/infants. A good model prediction requires a thorough understanding of the complex interplay between CYP maturation and inhibition in infants.

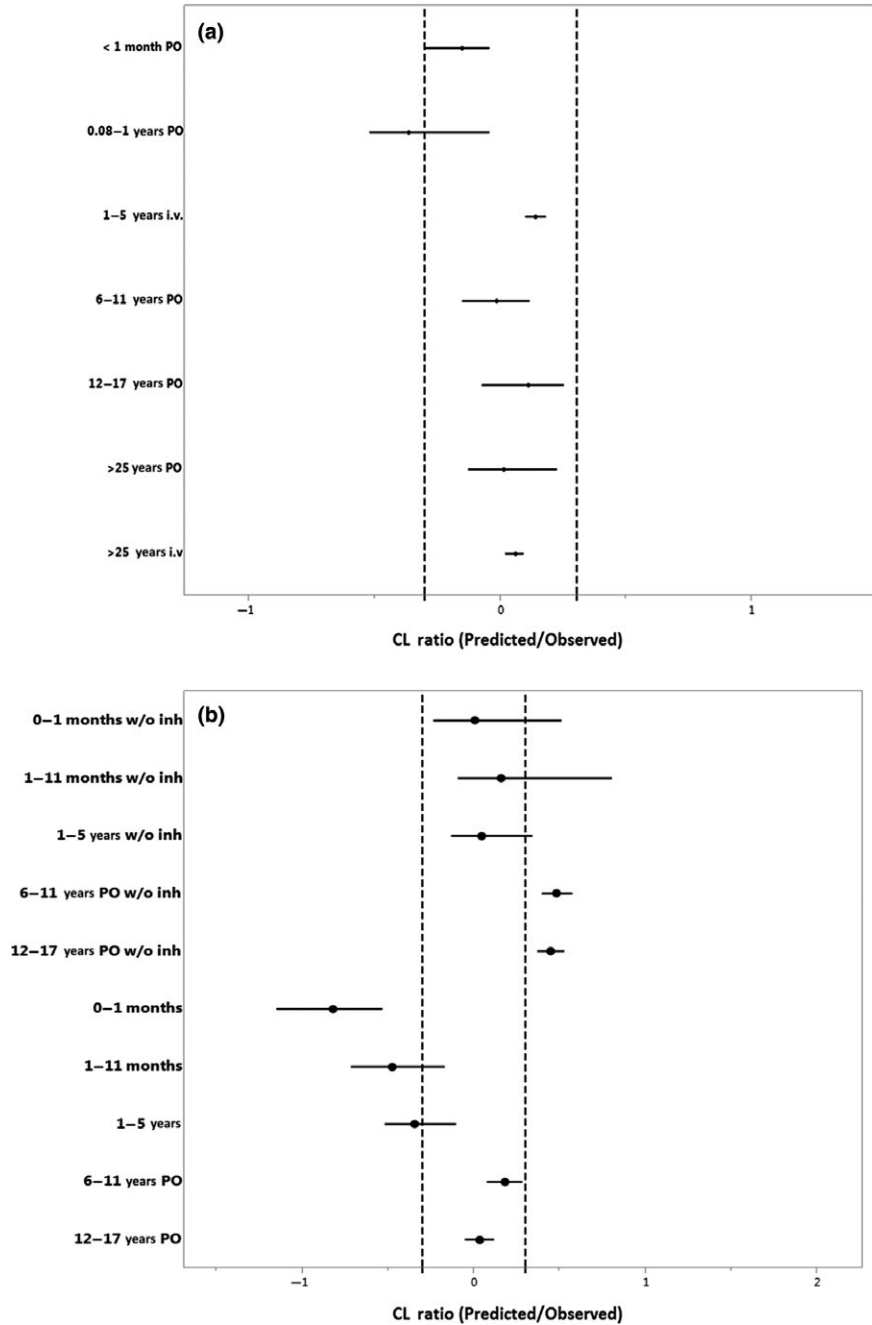


Figure 3 Comparison between pantoprazole (a) and esomeprazole (b) observed and predicted value of clearance (CL) ratio in adult and different age groups of pediatric populations. Results are presented as mean ratios (solid circles) in each age group with a 95% confidence interval (horizontal lines). The ratios in X-axis are shown in log scale. Dashed lines represent where ratio = -0.301 ($\text{Log}_{10} 0.5$) and 0.301 ($\text{Log}_{10} 2$), respectively. “w/o inh” indicates simulation without cytochrome P450 2C19 inhibition.

In auto-inhibition (mechanism-based enzyme inhibition), enzymes are irreversibly removed from the active enzyme pool, thus showing a prolonged inhibition upon removal of the inhibitor. The only way to recover the enzyme activity is through the *de novo* synthesis. CYP2C19 is minimally expressed in the fetus and neonates, and the level of CYP2C enzymes, including CYP2C19, is almost undetectable in the first 24 hours after birth.⁴⁴ The amount of CYP2C19

increases quickly after birth and reaches one third of the adult level after the first month of life.⁴⁴ It is possible that the quick *de novo* synthesis of CYP2C19 in neonates provides more active enzyme and compensates for the enzyme auto-inhibition by esomeprazole.

Our hypothesis is supported by significantly improved prediction of esomeprazole clearance in infants by not including the CYP2C19 auto-inhibition in the esomeprazole

PBPK model (“w/o inh” in **Figure 3b** and **Table S4**). It should be noted that there are other mechanisms that may contribute to the underprediction of esomeprazole clearance in infants, including different protein binding capacity between neonates/infants and adults,^{43,45} and a compensatory pathway mediated by CYP3A4 or other enzymes.⁴⁶

There are a few limitations for our study. The models developed in the study did not include preterm infants due to limited observed data and a poor understanding of human physiology and enzyme/transporter ontogeny in this subpopulation. In addition, *in vitro* data suggest that pantoprazole might be a substrate of P-glycoprotein (P-gp).¹⁹ The effect of P-gp on absorption is not considered in our current model due to the limited data regarding transporter maturation, and the contribution of P-gp to absorption may not be significant because pantoprazole is a high permeability compound. Furthermore, pantoprazole clearance after i.v. and oral administration is similar, suggesting that intestinal efflux transporter or enzyme metabolism is minimal compared to hepatic clearance. Experimental data on the interplay between CYP2C19 *de novo* synthesis and enzyme inhibition would corroborate our conclusion. However, due to the difficulty in conducting experiments in younger children, and especially neonates, the experimental data in the literatures are limited. Future *in vitro* or *in vivo* studies are warranted to further understand the complex enzyme maturation mechanisms.

In summary, this study demonstrated different predictive performance of PBPK models in the neonates and infants for pantoprazole and esomeprazole, two drugs that share the same metabolic CYP2C19 pathway. These observations suggest that there is a complex interplay among CYP2C19 maturation, inhibition, and possible compensatory pathways in neonates and infants. Models involving substrates for CYP2C19 cannot be extrapolated to other CYP2C19 substrates in neonates and infants without verification. This age-dependent interplay warrants further experimental investigation and modeling verification through the study of other CYP2C19 substrates and/or inhibitors.

Supporting Information. Supplementary information accompanies this paper on the *CPT: Pharmacometrics & Systems Pharmacology* website (www.psp-journal.com).

Table S1. Predicted or observed pantoprazole PK parameters in adult or pediatric population with different CYP2C19 genotype.

Table S2. Observed PK parameters of pantoprazole in adult and pediatric population (Mean ± SD).

Table S3. Predicted performance of the pantoprazole PBPK model in different pediatric age groups.

Table S4. Prediction of PK across pediatric age groups using the esomeprazole PBPK model with or without auto-inhibition⁶.

Funding. D.G. receives support for research from the National Institute of Child Health and Human Development (K23HD083465). J.M. was supported by NIH grant T32GM008562 during the drafting of the manuscript.

Conflict of Interest. The authors declared no competing interests for this work.

Author Contributions. P.D., F.W., J.N.M., J.F., V.C., D.G., G.J.B., L.Z., and J.W. wrote the manuscript. P.D., J.W., and F.W. designed the research. P.D., F.W., and J.N.J. performed the research. P.D., F.W., and J.N.J. analyzed the data.

Disclaimer. The opinions in this article reflect the views of the authors and should not be interpreted as the position of the US Food and Drug Administration.

1. van den Anker, J.N., Coppes, M.J. & Koren, G. Neonatal and pediatric clinical pharmacology. *Pediatr. Clin. North Am.* **59**, xv–xviii (2012).
2. Baber, N. & Pritchard, D. Dose estimation for children. *Br. J. Clin. Pharmacol.* **56**, 489–493 (2003).
3. Duan, P. et al. Physiologically based pharmacokinetic prediction of linezolid and emtricitabine in neonates and infants. *Clin. Pharmacokinet.* **56**, 383–394 (2017).
4. Laughon, M.M. et al. Drug labeling and exposure in neonates. *JAMA Pediatr.* **168**, 130–136 (2014).
5. Food and Drug Administration. Summary of Meeting Minutes for Advisory Committee for Pharmaceutical Science and Clinical Pharmacology <<http://www.fda.gov/downloads/AdvisoryCommittees/CommitteesMeetingMaterials/Drugs/AdvisoryCommitteeForPharmaceuticalScienceandClinicalPharmacology/UCM306989.pdf>>. Accessed 14 March 2012.
6. Johnson, T.N., Zhou, D. & Bui, K.H. Development of physiologically based pharmacokinetic model to evaluate the relative systemic exposure to quetiapine after administration of IR and XR formulations to adults, children and adolescents. *Biopharm. Drug Dispos.* **35**, 341–352 (2014).
7. Jiang, X.L., Zhao, P., Barrett, J.S., Lesko, L.J. & Schmidt, S. Application of physiologically based pharmacokinetic modeling to predict acetaminophen metabolism and pharmacokinetics in children. *CPT Pharmacometrics Syst. Pharmacol.* **2**, e80 (2013).
8. Leong, R. et al. Regulatory experience with physiologically based pharmacokinetic modeling for pediatric drug trials. *Clin. Pharmacol. Ther.* **91**, 926–931 (2012).
9. Maharaj, A.R. & Edginton, A.N. Physiologically based pharmacokinetic modeling and simulation in pediatric drug development. *CPT Pharmacometrics Syst. Pharmacol.* **3**, e150 (2014).
10. Zhao, P., Rowland, M. & Huang, S.M. Best practice in the use of physiologically based pharmacokinetic modeling and simulation to address clinical pharmacology regulatory questions. *Clin. Pharmacol. Ther.* **92**, 17–20 (2012).
11. Koukouritaki, S.B. et al. Developmental expression of human hepatic CYP2C9 and CYP2C19. *J. Pharmacol. Exp. Ther.* **308**, 965–974 (2004).
12. Scott, S.A. et al. PharmGKB summary: very important pharmacogene information for cytochrome P450, family 2, subfamily C, polypeptide 19. *Pharmacogenet. Genomics* **22**, 159–165 (2012).
13. Huber, R. et al. Pharmacokinetics of pantoprazole in man. *Int. J. Clin. Pharmacol. Ther.* **34**, S7–S16 (1996).
14. Drugs@FDA. Clinical Pharmacology and Biopharmaceutics Review for NDA 020987. <https://www.accessdata.fda.gov/drugsatfda_docs/nda/2000/20987_Protonix_biopharmr_P1.pdf>. Accessed 28 January 2000.
15. Barrett, J.S., Della Casa Alberighi, O., Laer, S. & Meibohm, B. Physiologically based pharmacokinetic (PBPK) modeling in children. *Clin. Pharmacol. Ther.* **92**, 40–49 (2012).
16. Maharaj, A.R., Barrett, J.S. & Edginton, A.N. A workflow example of PBPK modeling to support pediatric research and development: case study with lorazepam. *AAPS J.* **15**, 455–464 (2013).
17. Huber, R. et al. Pharmacokinetics of pantoprazole in man. *Int. J. Clin. Pharmacol. Ther.* **34**, 185–194 (1996).
18. Gawronska-Szklarz, B. et al. CYP2C19 polymorphism affects single-dose pharmacokinetics of oral pantoprazole in healthy volunteers. *Eur. J. Clin. Pharmacol.* **68**, 1267–1274 (2012).
19. Pauli-Magnus, C., Rekersbrink, S., Klotz, U. & Fromm, M.F. Interaction of omeprazole, lansoprazole and pantoprazole with P-glycoprotein. *Naunyn Schmiedebergers Arch. Pharmacol.* **364**, 551–557 (2001).
20. Drugs@FDA. Clinical Pharmacology and Biopharmaceutics Review for NDA 020988. <http://www.accessdata.fda.gov/drugsatfda_docs/nda/2001/20988_Protonix_biopharmr.pdf>. Accessed 30 June 1998
21. Rodgers, T., Leahy, D. & Rowland, M. Physiologically based pharmacokinetic modeling 1: predicting the tissue distribution of moderate-to-strong bases. *J. Pharm. Sci.* **94**, 1259–1276 (2005).
22. Rodgers, T. & Rowland, M. Physiologically based pharmacokinetic modelling 2: predicting the tissue distribution of acids, very weak bases, neutrals and zwitterions. *J. Pharm. Sci.* **95**, 1238–1257 (2006).
23. Rowland, M. & Tozer, T. *Clinical Pharmacokinetics: Concepts and Applications, Second edn.* (Lea and Febiger, London, 1989).
24. Meyer, U.A. Metabolic interactions of the proton-pump inhibitors lansoprazole, omeprazole and pantoprazole with other drugs. *Eur. J. Gastroenterol. Hepatol.* **8**(suppl. 1), S21–S25 (1996).

25. Kearns, G.L. *et al.* Single-dose pharmacokinetics of oral and intravenous pantoprazole in children and adolescents. *J. Clin. Pharmacol.* **48**, 1356–1365 (2008).
26. Vieira, M.L. *et al.* Predicting drug interaction potential with a physiologically based pharmacokinetic model: a case study of telithromycin, a time-dependent CYP3A inhibitor. *Clin. Pharmacol. Ther.* **91**, 700–708 (2012).
27. NDA 020987 PROTONIX Label. <https://www.accessdata.fda.gov/drugsatfda_docs/label/2017/020987s051,022020s013lbl.pdf> (2017).
28. Wu, F. *et al.* Predicting nonlinear pharmacokinetics of omeprazole enantiomers and racemic drug using physiologically based pharmacokinetic modeling and simulation: application to predict drug/genetic interactions. *Pharm. Res.* **31**, 1919–1929 (2014).
29. Ogilvie, B.W. *et al.* The proton pump inhibitor, omeprazole, but not lansoprazole or pantoprazole, is a metabolism-dependent inhibitor of CYP2C19: implications for coadministration with clopidogrel. *Drug Metab. Dispos.* **39**, 2020–2033 (2011).
30. Ward, R.M. *et al.* A multicenter, randomized, open-label, pharmacokinetics and safety study of pantoprazole tablets in children and adolescents aged 6 through 16 years with gastroesophageal reflux disease. *J. Clin. Pharmacol.* **51**, 876–887 (2011).
31. James, L. *et al.* Pharmacokinetics and tolerability of rabeprazole sodium in subjects aged 12 to 16 years with gastroesophageal reflux disease: an open-label, single- and multiple-dose study. *Clin. Ther.* **29**, 2082–2092 (2007).
32. Tammarra, B.K. *et al.* Randomized, open-label, multicentre pharmacokinetic studies of two dose levels of pantoprazole granules in infants and children aged 1 month through <6 years with gastro-oesophageal reflux disease. *Clin. Pharmacokinet.* **50**, 541–550 (2011).
33. Ward, R.M. *et al.* Single-dose, multiple-dose, and population pharmacokinetics of pantoprazole in neonates and preterm infants with a clinical diagnosis of gastroesophageal reflux disease (GERD). *Eur. J. Clin. Pharmacol.* **66**, 555–561 (2010).
34. Johnson, T.N., Rostami-Hodjegan, A. & Tucker, G.T. Prediction of the clearance of eleven drugs and associated variability in neonates, infants and children. *Clin. Pharmacokinet.* **45**, 931–956 (2006).
35. Barter, Z.E. *et al.* Scaling factors for the extrapolation of in vivo metabolic drug clearance from in vitro data: reaching a consensus on values of human microsomal protein and hepatocellularity per gram of liver. *Curr. Drug Metab.* **8**, 33–45 (2007).
36. Barter, Z.E. *et al.* Covariation of human microsomal protein per gram of liver with age: absence of influence of operator and sample storage may justify interlaboratory data pooling. *Drug Metab. Dispos.* **36**, 2405–2409 (2008).
37. von Richter, O. *et al.* Cytochrome P450 3A4 and P-glycoprotein expression in human small intestinal enterocytes and hepatocytes: a comparative analysis in paired tissue specimens. *Clin. Pharmacol. Ther.* **75**, 172–183 (2004).
38. Shiran, M.R. *et al.* Prediction of metabolic drug clearance in humans: in vitro-in vivo extrapolation vs allometric scaling. *Xenobiotica* **36**, 567–580 (2006).
39. Fieller, E.C. Some problems in interval estimation. *J. R. Stat. Soc.* **16**, 175–185 (1954).
40. Sager, J.E., Yu, J., Ragueneau-Majlessi, I. & Isoherranen, N. Physiologically based pharmacokinetic (PBPK) modeling and simulation approaches: a systematic review of published models, applications, and model verification. *Drug Metab. Dispos.* **43**, 1823–1837 (2015).
41. Chetty, M. *et al.* Prediction of the pharmacokinetics, pharmacodynamics, and efficacy of a monoclonal antibody, using a physiologically based pharmacokinetic FcRn model. *Front Immunol.* **5**, 670 (2014).
42. Sandstrom, M. *et al.* Phase I, multicenter, randomized, open-label study evaluating the pharmacokinetics and safety profile of repeated once-daily doses of intravenous esomeprazole in children 0 to 17 years of age. *Clin. Ther.* **34**, 1828–1838 (2012).
43. Calvier, E.A.M. *et al.* Drugs being eliminated via the same pathway will not always require similar pediatric dose adjustments. *CPT Pharmacometrics Syst. Pharmacol.* **7**, 175–185 (2018).
44. Oesterheld, J.R. A review of developmental aspects of cytochrome P450. *J. Child. Adolesc. Psychopharmacol.* **8**, 161–174 (1998).
45. Zhou, W. *et al.* Predictive performance of physiologically based pharmacokinetic (PBPK) modeling of drugs extensively metabolized by major cytochrome P450s in children. *Clin. Pharmacol. Ther.* **104**, 188–200 (2017).
46. Pacifici, G.M. & Allegaert, K. Clinical pharmacology of paracetamol in neonates: a review. *Curr. Ther. Res. Clin. Exp.* **77**, 24–30 (2015).
47. Pue, M.A., Laroche, J., Meineke, I. & de Mey, C. Pharmacokinetics of pantoprazole following single intravenous and oral administration to healthy male subjects. *Eur. J. Clin. Pharmacol.* **44**, 575–578 (1993).
48. Hassan-Alin, M., Andersson, T., Bredberg, E. & Rohss, K. Pharmacokinetics of esomeprazole after oral and intravenous administration of single and repeated doses to healthy subjects. *Eur. J. Clin. Pharmacol.* **56**, 665–670 (2000).
49. Andersson, T. & Weidolf, L. Stereoselective disposition of proton pump inhibitors. *Clin. Drug Investig.* **28**, 263–279 (2008).
50. Hassan-Alin, M., Andersson, T., Niazi, M. & Rohss, K. A pharmacokinetic study comparing single and repeated oral doses of 20 mg and 40 mg omeprazole and its two optical isomers, S-omeprazole (esomeprazole) and R-omeprazole, in healthy subjects. *Eur. J. Clin. Pharmacol.* **60**, 779–784 (2005).

Published 2018. This article is a U.S. Government work and is in the public domain in the USA.
CPT: Pharmacometrics & Systems Pharmacology published by Wiley Periodicals, Inc. on behalf of the American Society for Clinical Pharmacology and Therapeutics. This is an openaccess article under the terms of the Creative Commons Attribution-NonCommercial License, which permits use, distribution and reproduction in any medium, provided the original work is properly cited and is not used for commercial purposes.